Direct reconstruction of complex refractive index distribution from boundary measurement of intensity and normal derivative of intensity

Hari M. Varma,[1] R. Mohan Vasu,[1,*] and A. K. Nandakumaran[2]

[1]*Department of Instrumentation*
[2]*Department of Mathematics, Indian Institute of Science, Bangalore 560 012, India*
[*]*Corresponding author: vasu@isu.iisc.ernet.in*

Received February 16, 2007; accepted June 5, 2007;
posted June 29, 2007 (Doc. ID 80160); published September 7, 2007

We present an optical tomographic reconstruction method to recover the complex refractive index distribution from boundary measurements based on intensity, which are the logarithm of intensity and normal derivative of intensity. The method, which is iterative, repeatedly implements the forward propagation equation for light amplitude, the Helmholtz equation, and computes appropriate sensitivity matrices for these measurements. The sensitivity matrices are computed by solving the forward propagation equation for light and its adjoint. The results of numerical experiments show that the data types $\ln(I)$ and $\partial I/\partial n$ reconstructed, respectively, the imaginary and the real part of the object refractive index distribution. Moreover, the imaginary part of the refractive index reconstructed from $\partial I/\partial n$ and the real part from $\ln(I)$ failed to show the object's inhomogeneity. The value of the propagation constant, k, used in our simulations was 50, and this value resulted in smoothing of the reconstructed inhomogeneities. Thus we have shown that it is possible to reconstruct the complex refractive index distribution directly from the measured intensity without having to first find the light amplitude, as is done in most of the currently available reconstruction algorithms of diffraction tomography.

OCIS codes: 050.1940, 110.6960, 290.3200.

1. INTRODUCTION

For the reconstruction of the complex refractive index of objects at a spatial resolution comparable with the wavelength of radiation used to interrogate the object, diffraction tomography is employed [1,2]. Diffraction tomography provides inversion algorithms based on the Fourier diffraction theorem, such as filtered backpropagation or the direct Fourier method, under the assumption of weak scattering. In addition to these noniterative methods, there are also iterative methods employed for solving the inverse problem, which have provisions to circumvent the weak scattering approximation [3,4,6]. Under these schemes, the Helmholtz equation is inverted either directly or indirectly, through repeated implementation of the forward operator and its adjoint, for recovering the complex refractive index distribution [6]. In these two methods the data on the boundary constitute the complex amplitude, which is the sum of the incident and the scattered field, and a complete data set should have both the intensity and phase of the transmitted light. Whereas the intensity is easily detected by photodetectors or CCD arrays, phase is not; phase detection requires indirect and experimentally complex measurement methods [7]. Phase recovery from the intensity measurement is also employed to retrieve the complex amplitude from the intensity data [8–10], which in turn is used in the noniterative diffraction tomographic algorithm to reconstruct the complex refractive index distribution [11]. One of the methods used for phase recovery uses the transport of intensity equation (TIE) [8], which is a partial differential equation connecting the wavefront (i.e., phase) to the axial transport of intensity (i.e., the normal derivative of the intensity).

Since a complete recovery of the complex amplitude data is cumbersome, there have been many attempts to reconstruct the refractive index distribution directly from the measured intensity data [12–14]. Under this category falls the method that treats the intensity recorded at the far field as a Gabor hologram [15], the reconstruction from which yields the correct refractive index along with its twin image and a constant intensity term. In another proposed method [13], which is close to the method proposed here, the complex refractive index distribution of the scattering objects with well-localized Fourier spectra are reconstructed from a number of intensity measurements on several planes. Here again the retrieval of the Fourier spectrum of the scattering object is dependent on its twin image's being either separated or small. (Smallness is ensured when the distance between the planes where the intensities are measured tends to zero).

In this work, we propose an iterative reconstruction procedure that successfully retrieves the real and imaginary parts of the complex refractive index from the measurement of the two data types derived from the complex amplitude at the boundary. The data types are the logarithm of intensity [$\ln(I)$] and the normal derivative of the intensity ($\partial I/\partial n$), which are intuitively selected keeping in mind the following facts: (i) the intensity of the transmitted light is affected primarily by the imaginary part of the object refractive index; (ii) the normal derivative of the in-

tensity, which determines the intensity transport across the wavefront, is controlled primarily by the curvature of the wavefront, which in turn is dependent on the real part of the refractive index of the object through which the light is propagated. The TIE itself has I and $\partial I/\partial n$ as parameters from which the phase of the wave is often reconstructed [16].

Accurate measurement of the normal derivative of intensity, $\partial I/\partial n$, is crucial in the practical application of TIE for phase recovery. This has been addressed in a number of recent publications [17–20]. The inverse problem addressed here, which is the direct recovery of the refractive index from $\ln(I)$ and $\partial I/\partial n$, is also critically dependent on accurate measurement of $\partial I/\partial n$ from I. For phase reconstruction using TIE, $\partial I/\partial z$, the axial intensity transport, which is $\partial I/\partial n$ for paraxial propagation of light along the z axis, is approximated by the finite-difference formula $[I_1(x,y,z+\mathrm{d}z)-I_2(x,y,z)]/\mathrm{d}z$. Here I_1 and I_2 are the intensities captured by a CCD array at the transverse plane $z+\mathrm{d}z$ and z, respectively. For a more accurate estimation of $\partial I/\partial z$ in the context of application in the TIE, $I(x,y,z)$ is measured at a number of transverse planes across the z axis from which I and $\partial I/\partial z$ are approximated through interpolation [20].

The reconstruction method presented here uses an iterative procedure similar to the so-called model-based iterative image reconstruction (MOBIIR) procedure of diffuse optical tomography (DOT) [21,22]. In DOT one makes use of different data types derived from the photon flux at the boundary. The types of data used in DOT are the intensity, expected time of arrival of a pulse, the amplitude and phase of the detected photon flux from an intensity-modulated illumination, etc. The MOBIIR algorithm repeatedly solves the forward problem and the perturbation equation connecting the change in the data to the change in the optical property through the Jacobian estimated for the particular data to be considered. In adapting this technique for the diffraction tomography problem at hand, data from each view (or projection), which are either $\ln(I)$ or $\partial I/\partial z$, are handled separately for reconstructing the refractive index, similar to the propagation–backpropagation strategy proposed and used in [6] in the context of ultrasound tomography. The components of the Jacobian here are the rate of the change of measurements, $\ln(I)$ and $\partial I/\partial z$, with respect to the discretized optical properties of the object in the pixels. The details of estimating the Jacobian are given in Appendix A.

One interesting aspect of our procedure is that we do not solve two boundary value problems to reconstruct an update vector, namely, the forward problem and the adjoint of the Frechet derivative of the forward operator as is done in [6]. Instead the adjoint is used for a quick estimation of the Jacobian of the forward operator, which is used in the perturbation equation of the forward operator connecting measurement changes to changes in the refractive index. This perturbation equation is solved to update the initial distribution.

The organization of the rest of the paper is as follows: in Section 2, we introduce the MOBIIR adapted to the recovery of the complex refractive index distribution from the intensity-based measurements. In Section 3, we introduce the forward propagation equation for light amplitude, based on the Helmholtz equation. The Jacobian calculation for the two data types is explained in Section 4. Section 5 describes the numerical experiments, where a simulated refractive index distribution is reconstructed by using the MOBIIR algorithm. Discussion of results and concluding remarks are in Section 6. The procedure used to estimate the Jacobian for the two measurements that employ the adjoint of the Frechet derivative of the forward propagation equation is described in Appendix A.

2. ITERATIVE RECONSTRUCTION ALGORITHM

The proposed reconstruction algorithm is shown in the block diagram of Fig. 1. There are two iterations, an inner and an outer, in the usual inversion that involves basically two major steps. The first step involves the implementation of the forward propagation equation, which computes an approximation to the experimental data given the optical properties (the complex refractive index) of the object. The forward propagation equation, which is based on the Helmholtz equation, is further discussed in Section 3. It computes the perturbation in the output complex amplitude u_s given the perturbation in the optical properties of the object. From this perturbation we can find the total complex field at the boundary by adding the input amplitude u_0, which is a plane wave. The data are computed from $u=u_0+u_s$, the total field at the boundary, and are (i) the logarithm of intensity I, which is $I=\langle|u_0+u_s|^2\rangle$, and (ii) the normal derivative of the intensity, $\partial I/\partial n$.

The second major step is the calculation of Jacobian matrix corresponding to the two data types of interest. One element of the Jacobian matrix for the data type

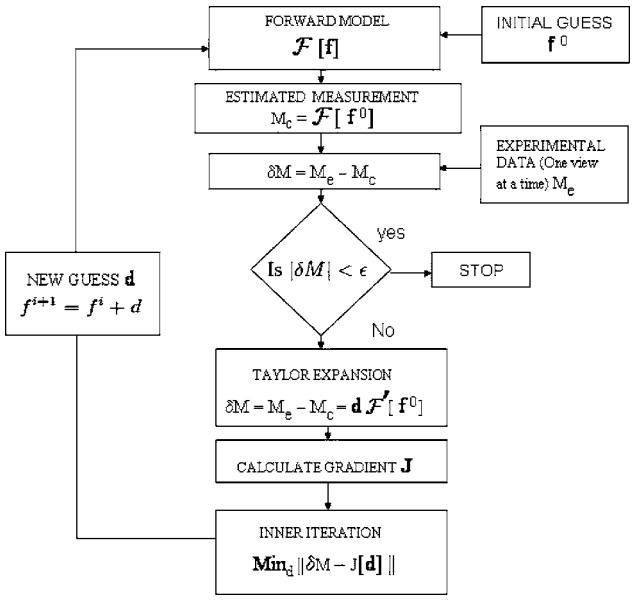

Fig. 1. MOBIIR algorithm: the inputs are the experimental measurement M_e and the initial guess of the optical property f^0. The algorithm has two iterative loops, the outer and the inner. In the outer loop, the perturbation equation is updated, and in the inner loop the perturbation equation is solved for the optical property distribution.

$\partial I/\partial n$ is the rate of change of $\partial I/\partial n$ with respect to the real or imaginary part of the refractive index at a particular node under consideration. If the object is discretized by using the finite-element method to N nodal values of the complex refractive index, the Jacobian for one measurement will have $2N$ elements consisting of derivatives with respect to real and imaginary parts of the refractive index at these nodes. The strategy of the inversion algorithm described in Fig. 1, which uses only the forward propagation equation and the Jacobian (or sensitivity matrix), is given below.

Given a set of experimental measurements $\ln(I) = \ln[\langle|u_0+u_s|^2\rangle]$ or $\partial I/\partial n$ corresponding to the different angles of illumination, the algorithm starts with an initial guess of the optical properties, for example, the background values. For these optical properties the measurements M_c are computed and compared with their experimental counterparts, M_e, and the perturbations $\Delta M = M_e - M_c$ are obtained. From the knowledge of the Jacobian evaluated at the current estimate of the optical properties, a perturbation equation $\Delta M = J \cdot [\Delta f]$ is set up connecting ΔM to a perturbation Δf in optical properties. A regularized and normalized version of the perturbation equation $J^T \Delta M = J^T \cdot J \cdot [\Delta f + \lambda \cdot I_d]$, where I_d is the identity matrix, is solved for Δf by minimizing the norm $\|J^T \Delta M - J^T \cdot J \cdot [\Delta f + \lambda \cdot I_d]\|^2$ with respect to f by using either a conjugate gradient scheme or a quasi-Newton algorithm. Here λ is the regularization parameter fixed by heuristic methods. This last iteration is represented by the inner loop in the reconstruction algorithm of Fig. 1. The Δf_i obtained from the inner loop is used to update the current optical properties as $f^{i+1} = f^i + \Delta f^i$, which are the inputs to the forward operator to continue the outer iteration. The Jacobian also needs to be recomputed, and the perturbation equation is updated with the current Jacobian and ΔM.

In the implementation of the MOBIIR algorithm we follow the strategy of splitting the perturbation equation into those pertaining to data from each view. One angle of input illumination gives data for a particular view. Once the perturbation equation for one view is solved for the refractive index distribution, it is updated and used to form the new perturbation equation pertaining to the data from the next view. When we have gone through the data from all views, the entire procedure is repeated, starting from the first view. The stopping criterion for the iteration is ensuring that the mean square error between M_e and M_c, i.e., $\|M_e - M_c\|^2$, has reached a minimum.

As is seen from the above discussion, the two major issues to be tackled are the implementation of the forward operator and the calculation of the Jacobian for the two data types $\ln(I)$ and $\partial I/\partial n$. The implementation of these two steps is described in the following sections.

3. IMPLEMENTATION OF THE FORWARD OPERATOR

The propagation of monochromatic wave of wavelength λ_0 through a medium of refractive index distribution $n(\mathbf{r})$ is governed by the Helmholtz equation

$$\nabla \cdot \nabla u(\mathbf{r}) + k^2 u(\mathbf{r}) = 0. \quad (1)$$

Here $u(\mathbf{r})$ is the complex amplitude of the wave and $k(\mathbf{r}) = n(\mathbf{r})(2\pi/\lambda_0)$ is the modulus of the propagation vector. Considering $n(\mathbf{r}) = 1 + n_\delta(\mathbf{r})$, where $n_\delta(\mathbf{r})$ is a small perturbation to the background medium, which is air, whose refractive index is 1, we can approximate Eq. (1) as

$$\nabla \cdot \nabla u(\mathbf{r}) + k_0^2 (1 - f(\mathbf{r})) u(\mathbf{r}) = 0, \quad (2)$$

where $f(\mathbf{r})$ is given by

$$f(\mathbf{r}) = -2n_\delta(\mathbf{r}), \quad k_0 = 2\pi/\lambda_0.$$

Here we point out that the approximation used does not preclude refractive index distributions disallowed under Born or Rytov approximations [5]. The approximation under which the Jacobian is estimated, i.e, $|u^\delta| \ll u_0$ (see Section 4) does not put any restriction on $f(\mathbf{r})$ but only on $d(\mathbf{r})$, the perturbation in $f(\mathbf{r})$. This is easily justified for reaching $f(\mathbf{r})$ from $f^0(\mathbf{r})$ through a large number of iterations.

The object, assumed to be 2D and square shaped with boundaries L, L^-, and L^+, as shown in Fig. 2, is illuminated with a plane wave $e^{ik_0 \mathbf{r}\cdot\theta}$. Here θ is the unit vector in the propagation direction given by

$$\theta = \begin{pmatrix} -\sin\phi \\ \cos\phi \end{pmatrix},$$

where $\mathbf{r} \in \mathbb{R}^2$ and ϕ is the angle of illumination. The total field $u(\mathbf{r})$ at any point in the medium is given by the sum of the incident wave $e^{ik_0 \mathbf{r}\cdot\theta}$ and the scattered wave $v(\mathbf{r})e^{ik_0 \mathbf{r}\theta}$; that is,

$$u(\mathbf{r}) = e^{ik_0 \mathbf{r}\cdot\theta}(1 + v(\mathbf{r})).$$

Therefore Eq. (2) can be rewritten as an equation connecting $f(\mathbf{r})$, the perturbation in the refractive index and $v(\mathbf{r})$:

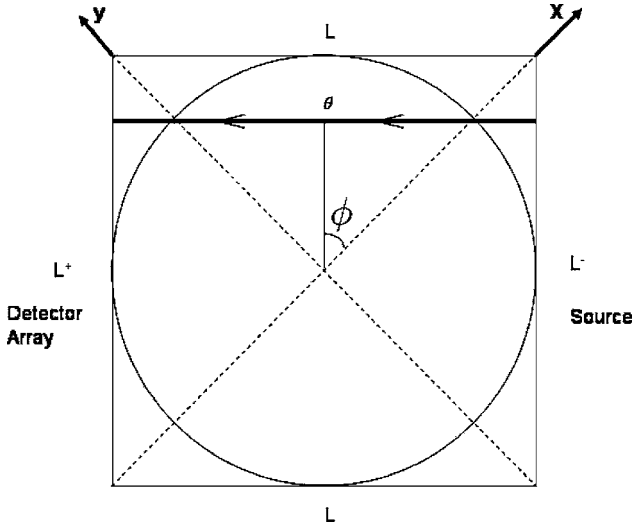

Fig. 2. Data collection geometry: the object, which is circular, is enclosed in a square region bounded by $L \cup L^- \cup L^+$. The source is a monochromatic plane wave incident on L^-, and the transmitted intensity is detected at L^+. Data for different views are gathered by rotating the circular region, which contains the inhomogeneity in refractive index.

$$\nabla \cdot \nabla v(\mathbf{r}) + 2ik_0\theta \cdot \nabla v(\mathbf{r}) - k_0^2 v(\mathbf{r}) f(\mathbf{r}) = k_0^2 f(\mathbf{r}). \quad (3)$$

Equation (3) is the forward propagation equation with the following boundary conditions:

$$v(\mathbf{r}) = g_\theta \text{ on } L, \quad v(\mathbf{r}) = 0 \text{ on } L^-, \quad (4)$$

$$v(\mathbf{r}) + \frac{\partial v(\mathbf{r})}{\partial n} = 0 \text{ on } L^+. \quad (5)$$

Here $\partial v(\mathbf{r})/\partial n$ is the normal derivative of $v(\mathbf{r})$ on L^+. The Robin boundary condition (5) on L^+ indicates that there is no boundary reflection of light allowed into the medium from L^+. The significance of the Dirichlet boundary condition on L^- is that backscattering is negligibly small, and therefore the scattered amplitude $v(\mathbf{r})$ reaching the boundary from where the illumination is put is zero [6].

The Frechet derivative operator corresponding to forward propagation equation (3) is obtained by substituting the perturbed scattered field $v(\mathbf{r})+v^\delta(\mathbf{r})$ and its cause, a perturbed object function $f(\mathbf{r})+d(\mathbf{r})$, into Eq. (3), which gives

$$\nabla \cdot \nabla v^\delta(\mathbf{r}) + 2ik_0\theta \cdot \nabla v^\delta(\mathbf{r}) - k_0^2 v^\delta(\mathbf{r}) f(\mathbf{r}) = k_0^2(1 + v(\mathbf{r}))d(\mathbf{r}). \quad (6)$$

The boundary conditions for the Frechet derivative of the forward propagation equation are

$$v^\delta(\mathbf{r}) = 0 \text{ on } L \cup L^-, \quad v^\delta(\mathbf{r}) + \frac{\partial v^\delta(\mathbf{r})}{\partial n} = 0 \text{ on } L^+. \quad (7)$$

Formally, we call the above operator the Frechet derivative of the forward propagation equation even though it solves for $v^\delta(\mathbf{r})$, the error in $v(\mathbf{r})$ caused by $d(\mathbf{r})$, an error in $f(\mathbf{r})$.

4. CALCULATION OF JACOBIAN FOR THE TWO DATA TYPES

For implementing the MOBIIR algorithm for each iteration, we need to update the computed data by solving the forward propagation equation for the current estimate of the refractive index and also the perturbation equation connecting the perturbation of the measurement to the perturbation of the refractive index through a suitable Jacobian (or sensitivity) matrix. As indicated earlier we employ two measurements derived from the total field measured on L^+ for various values of θ. They are the logarithm of intensity $I(\mathbf{r})$ and normal derivative of intensity $\partial I(\mathbf{r})/\partial n$. In the following we describe how the Jacobians are estimated for the two data types [23–26].

A. For Logarithm of Intensity

The measurement obtained from $u(\mathbf{r})$ is given by $\Gamma_I = \ln(u\bar{u})$. For evaluating the Jacobian one needs to arrive at the change Γ_I^δ in the measurement brought about by the change $d(\mathbf{r})$ in $f(\mathbf{r})$, the refractive index distribution. Assuming that $u(\mathbf{r})$ becomes $u(\mathbf{r})+u^\delta(\mathbf{r})$ when $f(\mathbf{r})$ becomes $f(\mathbf{r})+d(\mathbf{r})$, we can write Γ_I^δ as

$$\Gamma_I^\delta = \ln(u\bar{u} + u\bar{u}^\delta + u^\delta\bar{u} + u^\delta\bar{u}^\delta) - \ln(u\bar{u})$$
$$= \ln\left(\frac{u\bar{u} + u\bar{u}^\delta + u^\delta\bar{u} + u^\delta\bar{u}^\delta}{u\bar{u}}\right) \approx \ln\left(1 + \frac{u\bar{u}^\delta + u^\delta\bar{u}}{u\bar{u}}\right).$$

Assuming $|(u\bar{u}^\delta + u^\delta\bar{u})/u\bar{u}| \ll 1$, we get

$$\Gamma_I^\delta = \frac{u\bar{u}^\delta + u^\delta\bar{u}}{u\bar{u}} = \left(\frac{\bar{u}^\delta}{\bar{u}}\right) + \left(\frac{u^\delta}{u}\right).$$

The relation connecting u^δ and v^δ is given by

$$u^\delta = (1 + v + v^\delta)e^{ik_0\mathbf{r}\cdot\theta} - (1 + v)e^{ik_0\mathbf{r}\cdot\theta} = v^\delta e^{ik_0\mathbf{r}\cdot\theta}.$$

We notice that Γ_I^δ is real and has two terms (say $\Gamma_{I,1}^\delta$ and $\Gamma_{I,2}^\delta$), one being the complex conjugate of the other.

Contribution from $\Gamma_{I,1}^\delta = (1/u)\cdot v^\delta \cdot e^{ik_0\mathbf{r}\cdot\theta}$. We have

$$v^\delta = u\Gamma_{I,1}^\delta e^{-ik_0\mathbf{r}\cdot\theta}. \quad (8)$$

The Robin boundary condition on L^+ gives

$$\frac{\partial v^\delta}{\partial n} = -u\Gamma_{I,1}^\delta e^{-ik_0\mathbf{r}\cdot\theta}.$$

The adjoint operator of the Frechet derivative operator (6) is given by [6]

$$\nabla \cdot \nabla \psi(\mathbf{r}) + 2ik_0\theta \cdot \nabla \psi(\mathbf{r}) - k_0^2 \bar{f}(\mathbf{r})\psi(\mathbf{r}) = 0 \quad (9)$$

with boundary conditions

$$\frac{\partial \psi(\mathbf{r})}{\partial n} + \psi(\mathbf{r})(1 + 2ik_0\theta \cdot n) = q^+ \text{ on } L^+,$$

$$\psi(\mathbf{r}) = 0 \text{ on } L \cup L^-. \quad (10)$$

Here q^+ is a Robin source on the boundary L^+. Multiplying Eq. (6) by $\bar{\psi}$, integrating the product over the whole domain Ω, and using the Green's theorem and Eq. (9), we get the relation (after a short calculation)

$$\int_{L^+} \left[\frac{\partial \bar{\psi}}{\partial n} + \bar{\psi}(1 - 2ik_0\theta \cdot n)\right] \frac{\partial v^\delta}{\partial n} d^{n-1}\mathbf{r}$$
$$= \int_\Omega [k^2(1 + v(\mathbf{r}))d(\mathbf{r})]\bar{\psi}(\mathbf{r})\mathrm{d}^n\mathbf{r}.$$

Then for any Robin source q^+, we have

$$\int_{L^+} \left[\bar{q}^+ \frac{\partial v^\delta(\mathbf{r})}{\partial n}\right] \mathrm{d}^{n-1}\mathbf{r}$$
$$= \int_\Omega k_0^2(1 + v(\mathbf{r}))d(\mathbf{r})\bar{\psi}(\mathbf{r})\mathrm{d}^n\mathbf{r}. \quad (11)$$

When q^+ is a point source on the boundary $\partial\Omega$, the surface integral on the left-hand side of Eq. (11) picks up a measurement at that point only with strength given by $\partial v^\delta/\partial n$, which is related to the first part of the measurement through

$$\Gamma_{I,1}^{\delta} = -\frac{1}{u}\frac{\partial v^{\delta}}{\partial n} e^{ik_0 \mathbf{r}\cdot\theta},$$

where $\mathbf{r} \in \partial\Omega$. Therefore

$$\Gamma_{I,1}^{\delta}(\mathbf{m}_0) = -\frac{e^{ik_0 \mathbf{r}_{\mathbf{m}_0}}}{u(\mathbf{m}_0)} \int_{\Omega} k_0^2 (1 + v(\mathbf{r}')) d(\mathbf{r}') \bar{G}_R^{\psi}(\mathbf{r}', \mathbf{m}_0) \mathrm{d}^n \mathbf{r}'. \tag{12}$$

Here $\mathbf{r}_{\mathbf{m}_0} \equiv \mathbf{r}\cdot\theta$ for $\mathbf{r} = \mathbf{m}_0 \in L^+$ and $G_R^{\psi}(\mathbf{r}, \mathbf{m}_0)$ is the Green's function for the adjoint operator (9). But v^{δ} can be obtained from the Frechet derivative operator (6), through its Green's function as

$$v^{\delta}(\mathbf{m}_0) = \int_{\Omega} [G^{v}(\mathbf{m}_0, \mathbf{r}') k_0^2 (1 + v(\mathbf{r}')) d(\mathbf{r}') \mathrm{d}^n \mathbf{r}'].$$

Therefore

$$\Gamma_{I,1}^{\delta}(\mathbf{m}_0) = \frac{e^{ik_0 \mathbf{r}_{\mathbf{m}_0}}}{u(\mathbf{m}_0)} \int_{\Omega} k_0^2 (1 + v(\mathbf{r}')) d(\mathbf{r}') G^{\Gamma_{I,1}^{\delta}}(\mathbf{m}_0, \mathbf{r}') \mathrm{d}^n \mathbf{r}'. \tag{13}$$

Comparing Eqs. (12) and (13) and using the fact that the Robin source q^+ at the boundary picks out only the measurement at $\mathbf{m}_0$ on the boundary, we see that the solution ψ to Eq. (9) is an adjoint Green's function $G_R^{\psi}(\mathbf{r}', \mathbf{m}_0)$ with the property

$$G^{\Gamma_{I,1}^{\delta}}(\mathbf{m}_0, \mathbf{r}') = -\bar{G}_R^{\psi}(\mathbf{r}', \mathbf{m}_0). \tag{14}$$

This establishes the reciprocity relation that exists between the secondary sources at $\mathbf{r}'$ and the detector at $\mathbf{m}_0$, which is crucial in the quick estimation of the Jacobian.

Since $\Gamma_{I,2}^{\delta}$ is the complex conjugate of $\Gamma_{I,1}^{\delta}$, the expressions for $\Gamma_{I,2}^{\delta}$ are the complex conjugates of those given by Eqs. (12) and (13). The reciprocity relation can also be derived for $\Gamma_{I,2}^{\delta}$, which is

$$\bar{G}^{\Gamma_{I,2}^{\delta}}(\mathbf{m}_0, \mathbf{r}') = -G_R^{\psi}(\mathbf{r}', \mathbf{m}_0). \tag{15}$$

Therefore the sensitivity relation for $\Gamma_I^{\delta} = \Gamma_{I,1}^{\delta} + \Gamma_{I,2}^{\delta}$ is given by

$$\frac{\partial \Gamma_I(\mathbf{m}_0, \mathbf{r}')}{\partial d(\mathbf{r}')} = \frac{e^{ik_0 \mathbf{r}_{\mathbf{m}_0}}}{u(\mathbf{m}_0)} k_0^2 (1 + v(\mathbf{r}')) G^{\Gamma_{I,1}^{\delta}}(\mathbf{m}_0, \mathbf{r}') + \frac{e^{-ik_0 \mathbf{r}_{\mathbf{m}_0}}}{\bar{u}(\mathbf{m}_0)} k_0^2 (1 + \bar{v}(\mathbf{r}')) \bar{G}^{\Gamma_{I,2}^{\delta}}(\mathbf{m}_0, \mathbf{r}'). \tag{16}$$

The reciprocity relations in Eqs. (14) and (15) can be used to estimate the derivative $\partial \Gamma_I(\mathbf{m}_0, \mathbf{r}')/\partial d(\mathbf{r}')$ at all points $\mathbf{r}' \in \Omega$ simultaneously by estimating $G_R^{\psi}(\mathbf{r}', \mathbf{m}_0)$, the Green's function for the adjoint form of the Frechet derivative operator for a Robin source at $\mathbf{m}_0$ and $v(\mathbf{r}')$, the solution of Eq. (3).

B. Normal Derivative of Intensity

The second measurement obtained from $u(\mathbf{r})$ is $\Gamma_N = \partial I/\partial n$ at L^+ where n is the unit vector normal to L^+. For evaluating the Jacobian, we need the change in measurement Γ_N^{δ} due to the change $d(\mathbf{r})$ in $f(\mathbf{r})$, which is given by

$$\Gamma_N^{\delta} = \frac{\partial [u\bar{u}^{\delta} + u^{\delta}\bar{u} + u^{\delta}\bar{u}^{\delta}]}{\partial n}.$$

Since u^{δ} is very small, $u^{\delta}\bar{u}^{\delta}$ can be neglected compared with the other terms, which gives

$$\Gamma_N^{\delta} = \frac{\partial [u\bar{u}^{\delta} + u^{\delta}\bar{u}]}{\partial n}.$$

Expanding and rearranging, we get

$$\Gamma_N^{\delta} = \bar{u}\frac{\partial u^{\delta}}{\partial n} + \bar{u}^{\delta}\frac{\partial u}{\partial n} + u\frac{\partial \bar{u}^{\delta}}{\partial n} + u^{\delta}\frac{\partial \bar{u}}{\partial n}$$

$$= \Gamma_{N,1}^{\delta} + \Gamma_{N,2}^{\delta} + \Gamma_{N,3}^{\delta} + \Gamma_{N,4}^{\delta}. \tag{17}$$

As $\Gamma_{N,3}^{\delta} = \bar{\Gamma}_{N,1}^{\delta}$ and $\Gamma_{N,4}^{\delta} = \bar{\Gamma}_{N,2}^{\delta}$, the change in measurement Γ_N^{δ} is a real quantity.

1. Contribution from the First Term $\Gamma_{N,1}^{\delta}$ and Pertinent Reciprocity Relation

Using the relation between u^{δ} and v^{δ}, it is easy to see that

$$\Gamma_{N,1}^{\delta} = \bar{u}\frac{\partial [v^{\delta} e^{ik_0 \mathbf{r}\cdot\theta}]}{\partial n}.$$

Expanding, rearranging, and using Eq. (7), we get

$$\frac{\partial v^{\delta}}{\partial n} = \frac{\Gamma_{N,1}^{\delta} - v^{\delta}\bar{u}\dfrac{\partial [e^{ik_0 \mathbf{r}\cdot\theta}]}{\partial n}}{\bar{u} e^{ik_0 \mathbf{r}\cdot\theta}}$$

$$= \frac{\Gamma_{N,1}^{\delta} + \dfrac{\partial v^{\delta}}{\partial n}\bar{u}\dfrac{\partial [e^{ik_0 \mathbf{r}\cdot\theta}]}{\partial n}}{\bar{u} e^{ik_0 \mathbf{r}\cdot\theta}}. \tag{18}$$

The term $\partial [e^{ik_0 \mathbf{r}\cdot\theta}]/\partial [n]$ can be evaluated as follows: considering the normal direction at L^+ along the y axis and $\theta = (-\sin\phi, \cos\phi)$, we have

$$\frac{\partial [e^{ik_0 \mathbf{r}\cdot\theta}]}{\partial n} = e^{ik_0 \mathbf{r}\cdot\theta} ik_0 \cos\phi.$$

Using the above relation, $\partial v^{\delta}/\partial n$ restricted to L^+ can be obtained as

$$\left[\frac{\partial v^{\delta}}{\partial n}\right]\Bigg|_{L^+} = \frac{\Gamma_{N,1}^{\delta}}{\bar{u} e^{ik_0 \mathbf{r}\cdot\theta}} \left[\frac{1}{1 - ik_0 \cos\phi}\right].$$

Substituting into Eq. (11) and taking q^+ as a point source at $\mathbf{m}_0$, we have

$$\Gamma_{N,1}^{\delta}(\mathbf{m}_0) = e^{ik_0 \mathbf{r}_{\mathbf{m}0}} \bar{u}(\mathbf{m}_0)[1 - ik_0 \cos\phi] \times \int_{\Omega} k_0^2 (1 + v(\mathbf{r}')) d(\mathbf{r}') \bar{G}_R^{\psi}(\mathbf{r}', \mathbf{m}_0) \mathrm{d}^n \mathbf{r}'. \tag{19}$$

But v^{δ} can be expressed in terms of the Green's function solution for the equation for the Frechet derivative as

$$v^{\delta}(\mathbf{m}_0) = \int_{\Omega} [G^{v}(\mathbf{m}_0,\mathbf{r}')k_0^2(1+v(\mathbf{r}'))d(\mathbf{r}')]\mathrm{d}^n\mathbf{r}'.$$

Therefore the change in the first term of measurement $\Gamma^{\delta}_{N,1}(\mathbf{m}_0)$, in terms of the Green's function, is

$$\Gamma^{\delta}_{N,1}(\mathbf{m}_0) = \bar{u}(\mathbf{m}_0)e^{ik_0\mathbf{r}_{\mathbf{m}_0}}(1-ik_0\cos\phi) \times \int_{\Omega} G^{\Gamma_{N,1}}(\mathbf{m}_0,\mathbf{r}')k_0^2(1+v(\mathbf{r}'))d(\mathbf{r}')\mathrm{d}^n\mathbf{r}'. \tag{20}$$

Comparing Eqs. (19) and (20), as above, we have the following reciprocity relation with respect to $\Gamma^{\delta}_{N,1}$:

$$\bar{G}^{\psi}_{R}(\mathbf{r}',\mathbf{m}_0) = G^{\Gamma_{N,1}}(\mathbf{m}_0,\mathbf{r}'). \tag{21}$$

2. Contribution from the Second term $\Gamma^{\delta}_{N,2}$ and Reciprocity Relation

The second term in the measurement is

$$\Gamma^{\delta}_{N,2} = \frac{\partial u}{\partial n}\bar{u}^{\delta}.$$

Using the relation connecting u^{δ} and v^{δ}, we have

$$v^{\delta} = \frac{\bar{\Gamma}^{\delta}_{N,2}e^{-ik_0\mathbf{r}\cdot\theta}}{\partial\bar{u}/\partial n}.$$

Following a procedure similar to the one adopted in the previous subsection, we can derive the expressions for $\Gamma^{\delta}_{N,2}(\mathbf{m}_0)$ starting from Eqs. (9) and (10) (adjoint of the Frechet derivative) or Eqs. (3), (6), and (7) (the Frechet derivative operator itself). They are

$$\Gamma^{\delta}_{N,2}(\mathbf{m}_0) = -e^{-ik_0\mathbf{r}_{\mathbf{m}_0}}\frac{\partial u(\mathbf{m}_0)}{\partial n} \times \int_{\Omega} k_0^2(1+\bar{v}(\mathbf{r}'))\bar{d}(\mathbf{r}')G^{\psi}_{R}(\mathbf{r}',\mathbf{m}_0)\mathrm{d}^n\mathbf{r}', \tag{22}$$

$$\Gamma^{\delta}_{N,2}(\mathbf{m}_0) = -\frac{\partial u(\mathbf{m}_0)}{\partial n}e^{-ik_0\mathbf{r}_{\mathbf{m}_0}} \times \int_{\Omega} \bar{G}^{\Gamma_{N,2}}(\mathbf{m}_0,\mathbf{r}')k_0^2(1+\bar{v}(\mathbf{r}'))\bar{d}(\mathbf{r}')\mathrm{d}^n\mathbf{r}'. \tag{23}$$

Comparing Eqs. (22) and (23), we arrive at the reciprocity relation of the second term $\Gamma^{\delta}_{N,2}$,

$$G^{\psi}_{R}(\mathbf{r}',\mathbf{m}_0) = \bar{G}^{\Gamma_{N,2}}(\mathbf{m}_0,\mathbf{r}'). \tag{24}$$

The third part, given by $\Gamma^{\delta}_{N,3}(\mathbf{m}_0)=u(\partial\bar{u}^{\delta}/\partial n)$, is the complex conjugate of the first part, and therefore the expression for change in the measurement, $\Gamma^{\delta}_{N,3}(\mathbf{m}_0)$, is given by

$$\Gamma^{\delta}_{N,3}(\mathbf{m}_0) = e^{-ik_0\mathbf{r}_{\mathbf{m}_0}}u(\mathbf{m}_0)[1+ik_0\cos\phi] \times \int_{\Omega} k_0^2(1+\bar{v}(\mathbf{r}'))\bar{d}(\mathbf{r}')G^{\psi}_{R}(\mathbf{r}',\mathbf{m}_0)\mathrm{d}^n\mathbf{r}'. \tag{25}$$

The reciprocity relation obtained here is

$$G^{\psi}_{R}(\mathbf{r}',\mathbf{m}_0) = \bar{G}^{\Gamma_{N,3}}(\mathbf{m}_0,\mathbf{r}'). \tag{26}$$

Similarly, the fourth term $\Gamma^{\delta}_{N,4}=u^{\delta}(\partial\bar{u}/\partial n)$ is the complex conjugate of the second term, and therefore the change in measurement, $\Gamma^{\delta}_{N,4}(\mathbf{m}_0)$, is given by

$$\Gamma^{\delta}_{N,4}(\mathbf{m}_0) = -e^{ik_0\mathbf{r}_{\mathbf{m}_0}}\frac{\partial\bar{u}(\mathbf{m}_0)}{\partial n} \times \int_{\Omega} k_0^2(1+v(\mathbf{r}'))d(\mathbf{r}')\bar{G}^{\psi}_{R}(\mathbf{r}',\mathbf{m}_0)\mathrm{d}^n\mathbf{r}'. \tag{27}$$

The reciprocity relation is

$$\bar{G}^{\psi}_{R}(\mathbf{r}',\mathbf{m}_0) = G^{\Gamma_{N,4}}(\mathbf{m}_0,\mathbf{r}'). \tag{28}$$

Combining Eqs. (20), (22), (25), and (27) and the reciprocity relations, the sensitivity relation for the measurement Γ_N is given by

$$\begin{aligned}\frac{\partial\Gamma_N(\mathbf{m}_0,\mathbf{r}')}{\partial d(\mathbf{r}')} &= e^{ik_0\mathbf{r}_{\mathbf{m}0}}\bar{u}(\mathbf{m}_0)k_0^2(1-ik_0\cos\phi)(1+v(\mathbf{r}')) \times G^{\Gamma_{N,1}}(\mathbf{m}_0,\mathbf{r}') - e^{-ik_0\mathbf{r}_{\mathbf{m}_0}}\frac{\partial u(\mathbf{m}_0)}{\partial n}k_0^2(1+\bar{v}(\mathbf{r}')) \\ &\times \bar{G}^{\Gamma_{N,2}}(\mathbf{m}_0,\mathbf{r}') - e^{ik_0\mathbf{r}_{\mathbf{m}_0}}\frac{\partial\bar{u}(\mathbf{m}_0)}{\partial n}k_0^2(1+v(\mathbf{r}')) \\ &\times G^{\Gamma_{N,3}}(\mathbf{m}_0,\mathbf{r}') + u(\mathbf{m}_0)e^{-ik_0\mathbf{r}_{\mathbf{m}_0}}k_0^2 \\ &\times (1+ik_0\cos\phi)(1+\bar{v}(\mathbf{r}'))\bar{G}^{\Gamma_{N,4}}(\mathbf{m}_0,\mathbf{r}').\end{aligned} \tag{29}$$

The Jacobian matrix that contains elements of type $\partial\Gamma_I(\mathbf{m}_0,\mathbf{r}')/\partial d(\mathbf{r}')$ and $\partial\Gamma_N(\mathbf{m}_0,\mathbf{r}')/\partial d(\mathbf{r}')$ for all nodal points $\mathbf{r}'\in\Omega$ can be estimated by using Eqs. (16) and (29). In this, one can employ the reciprocity relations (21), (24), (26), and (28) and replace Green's function $G(\mathbf{m}_0,\mathbf{r}')$ by $G^{\psi}_{R}(\mathbf{r}',\mathbf{m}_0)$. The terms $G^{\psi}_{R}(\mathbf{r}',\mathbf{m}_0)$ can be evaluated for all nodal points $\mathbf{r}'\in\Omega$ by solving the adjoint of the Frechet derivative operator given by Eqs. (9) and (10) for a Robin source at $\mathbf{m}_0$. Apart from this, to compute Eqs. (16) and (29) we need $v(\mathbf{r}')$, the solution of the forward propagation equation at $\mathbf{r}'$. Therefore the derivative estimation using the adjoint of the Frechet derivative operator and the reciprocity relation involves the following steps:

1. For a particular illumination angle θ, solve the Frechet derivative operator given by Eqs. (6) and (7).
2. For a detector position $\mathbf{m}_0\in L^+$, solve the adjoint operator, i.e., Eqs. (9) and (10).
3. Compute the derivatives by using Eqs. (16) and (29).

5. NUMERICAL EXPERIMENTS

The object is square shaped (Fig. 2) and of dimensions 0.08×0.08 m. The background refractive index is $1+i0$ and has two inhomogeneous inclusions at $(x_1,y_1)=(0.025,0.04)$ and $(x_2,y_2)=(0.055,0.04)$. The first inhomogeneity is real and is of value $1.001+j0$, and the second is imaginary, which is $1+j0.001$. These are represented by a perturbation $f(x,y)$ given by

$$f(x,y)=\begin{cases} 0.001 & \text{if } \sqrt{(x-0.025)^2+(y-0.04)^2} \le 0.008 \\ 0.001i & \text{if } \sqrt{(x-0.055)^2+(y-0.04)^2} \le 0.008. \\ 0 & \text{otherwise} \end{cases}$$

The region of interest for reconstruction is a circle inscribed inside the square as shown in Fig. 2. The illumination direction θ is changed by rotating the inscribed circle containing the inhomogeneities. The illumination is a plane wave always from the boundary L^- and parallel to the sides. The data $\ln(I)$ and $\partial I/\partial n$ are generated for various angles of illumination by solving the forward propagation equation (3) with boundary conditions (4) and (5) for the total field u on L^+.

As mentioned in Section 1, the iterative procedure used here employs a variant of the propagation–backpropagation strategy used in [6]. In [6] the adjoint of the forward equation is implemented for backpropagating the data. Under the assumption that $|k_0|$ is very large the adjoint equation approximates the inverse of the forward equation. Therefore in [6] one has a generalization of the simultaneous algebraic reconstruction technique of x-ray tomography with the update for a particular view obtained through solving the adjoint of the Frechet derivative. With the updated optical properties the computed data for the next view is generated, and the algorithm proceeds by handling the data for this view to arrive at a new update vector. Here the spirit of propagation–backpropagation strategy is retained, but with a modification. The modification is that the adjoint of the Frechet derivative is used to compute the Jacobian of the forward propagation equation, which in turn is used to arrive at the perturbation equation (see Fig. 1). The perturbation equation is inverted, by using another iteration, to compute the update vector. This update vector generates the new estimate of the object, which is used to continue the algorithm, with the data from the next view.

The MOBIIR algorithm shown in Fig. 1 is implemented. The details are as follows: by the finite-element method the object described above is discretized to 1089 nodes and 2048 elements. The simulated experimental data is obtained by implementing the forward propagation equation with a finer mesh (4225 nodes, 8192 elements) for 36 views. The value of the modulus of the propagation vector k_0 used when solving the propagation equation, while either generating data or implementing the MOBIIR algorithm, is 50. A 1% Gaussian noise is added to data from each view. Implementation of one full

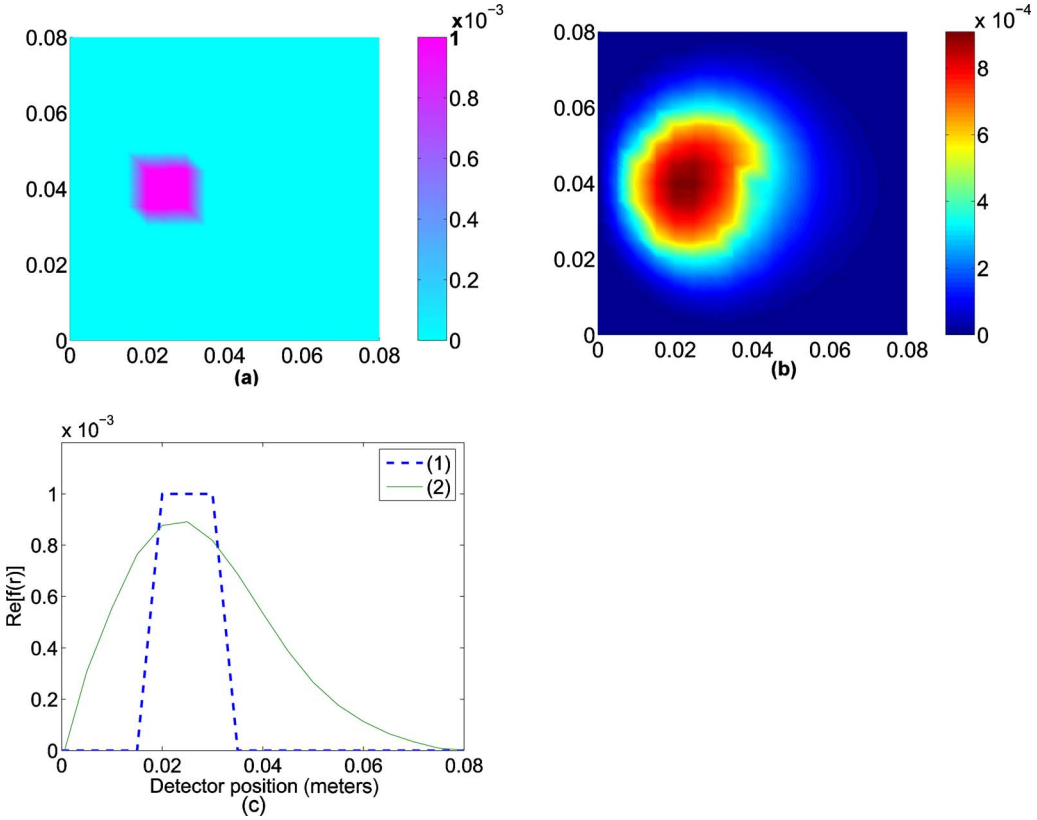

Fig. 3. (Color online) (a) Real part of the input object refractive index distribution. (b) Reconstructed image obtained from the normal derivative of the measured intensity at the boundary. (c) Cross-sectional plots through the center of the reconstruction in (a), curve (2) and the original object, curve (1).

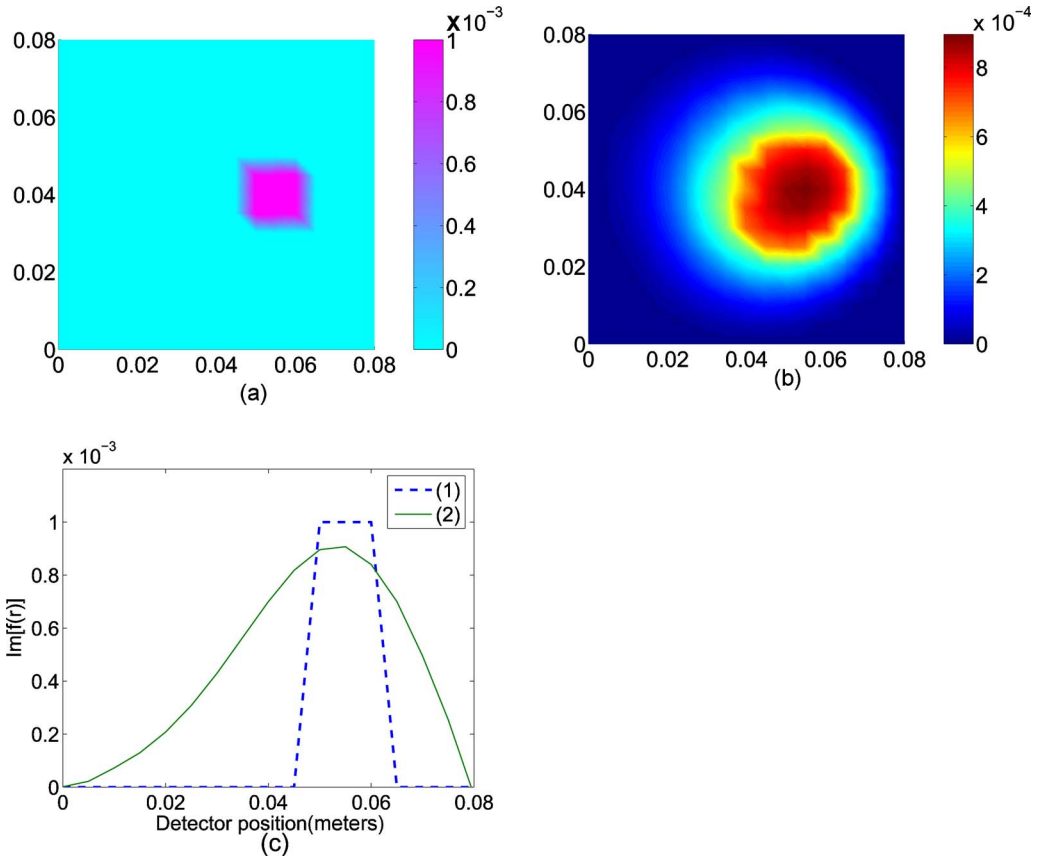

Fig. 4. (Color online) (a) Imaginary part of the input object refractive index distribution. (b) Reconstructed image obtained from the logarithm of the measured intensity at the boundary. (c) Cross-sectional plots through the center of the reconstruction in (a), curve (2) and the original object, curve (1).

iteration i.e, inverting data from all 36 views, took 612 s in a personal computer with a Pentium 4, 3 GHz processor. The algorithm generally converged in 35 iterations, with convergence indicated by $\|\delta M\| < \epsilon$, a small preset error.

The Jacobians corresponding to $\ln(I)$ and $\partial I/\partial n$ are constructed by using the procedure described in Section 4. Since the number of nodes is 1089 and the number of detectors on L^+ is 32, the Jacobians are of dimension 32×1089 for either the real or the imaginary part of the refractive index.

The reconstructions, which are complex, for both $\ln(I)$ and $\partial I/\partial n$ are predominantly biased toward either the imaginary part [for $\ln(I)$ data] or the real part [for $\partial I/\partial n$ data] of the refractive index distribution. Reconstruction from $\ln(I)$ indeed had a real part, just as the reconstruction from $\partial I/\partial n$ had an imaginary part, both of which were very small, less than 10% compared with their predominant counterpart. The real part of the refractive index obtained from $\partial I/\partial n$ and the imaginary part obtained from $\ln(I)$ are shown in Figs. 3 and 4. The results are discussed further in the next section.

6. RESULTS, DISCUSSION, AND CONCLUSIONS

The reconstructions shown in Figs. 3 and 4 are the real and the imaginary parts of the object refractive index inhomogeneity reconstructed from $\partial I/\partial n$ and $\ln(I)$, respectively. The maximum value of the reconstructed inhomogeneity is within 15% of its actual value. The reconstructions are spread over a large area around the inhomogeneity, and this due to the low value of k_0 used in the forward propagation equations.

Figure 5 shows the real part of the refractive index reconstructed from $\partial I/\partial n$ and $\ln(I)$, and Fig. 6 the imaginary part reconstructed from these two data types. These show that the data $\partial I/\partial n$ and $\ln(I)$ preferentially reconstruct the real and the imaginary parts of the refractive index,

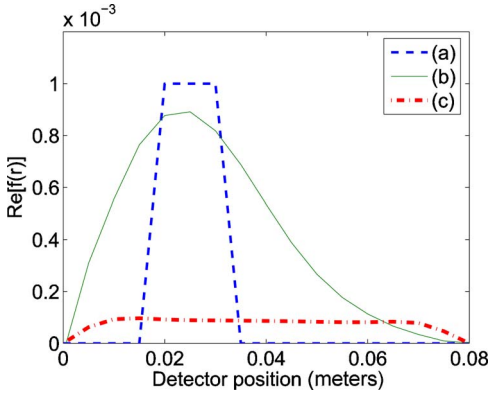

Fig. 5. (Color online) Cross section through the center of the inhomogeneity of the reconstructions from $\partial I/\partial n$. Curve (a), for real part of the original object; curve (b), real part of the reconstructed refractive index; curve (c), imaginary part of the reconstructed refractive index.

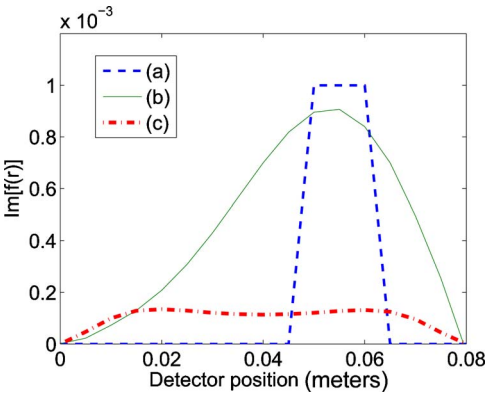

Fig. 6. (Color online) Cross section through the center of the inhomogeneity of the reconstructions from ln(I). Curve (a), imaginary part of the original object; curve (b), imaginary part of the reconstructed refractive index; curve (c), real part of the reconstructed refractive index.

and their spillover to imaginary and real parts, respectively, is small (less than 10%). The MOBIIR algorithm employed here is computationally more expensive than the propagation–backpropagation algorithm of [6]. However, since our data are related to the intensity, in the absence of a propagation equation for intensity this is the best adaptation of the algorithm of [6] to implement a reconstruction from data based on intensity.

For practical application of this method for diffraction tomographic reconstruction of the refractive index from light intensity measurements, it is necessary to implement the forward propagation equation with large k_0. The implementation of the Helmholtz equation for large k_0 values is difficult and was investigated by many in the past. The attempts include (i) the one-step Galerkin approximation employing generalized Jacobi approximation results (here explicit knowledge of continuous or discretized Green's function is not required) [27], (ii) a specially developed boundary element method in which the approximation space is designed to take care of the oscillating behavior of the Helmholtz equation for large k_0 [28], (iii) employing an asymptotic decomposition of the wave fields to arrive at the high-frequency solution [29], (iv) using appropriately designed marching schemes used to solve wave and Maxwell's equations [30], and (v) wavelet-based methods to decompose the high-frequency problems into low-frequency subproblems [31]. We are currently studying these methods to develop an efficient, stable, and accurate forward solver for use in the iterative inversion procedure developed in this work. Since we use visible or near-infrared light, a high-frequency solution for the Helmholtz equation is necessary to reconstruct the refractive index distribution of objects of practical interest of dimensions 10^5–10^6 times the wavelength. We are currently attempting a wavelet-based multiscale decomposition of the forward problem into a number of subproblems. Each of these subproblems effectively requires only a small wave number and therefore can be solved by one of the methods mentioned above. With this modification we believe that it is possible to have a scheme to reconstruct the complex refractive index distribution from data that are dependent only on light intensity measurement.

APPENDIX A: QUICK ESTIMATION OF THE JACOBIAN WHEN THE MEASUREMENT IS THE SCATTERED FIELD $v(\mathbf{r})$

Here we put forth a method for the quick estimation of the Jacobian when the measurement is $v(\mathbf{r})$. This is quick compared with the methods that rely on the forward propagation operator alone or those that make use of the Feynmann diagram, as is done in diffuse optical tomography [23]. The method presented here uses the adjoint form of the Frechet derivative given by Eq. (A1), which is derived here by using the same argument and methods used in [23] in the context of DOT.

As is seen in the main text the equation for estimating the perturbation in the scattered field, $v^\delta(\mathbf{r})$, that is due to a perturbation $d(\mathbf{r})$ in the object refractive index $f(\mathbf{r})$ is given by

$$\nabla\cdot\nabla v^\delta(\mathbf{r}) + 2ik_0\theta\cdot\nabla v^\delta(\mathbf{r}) - k_0^2 v^\delta(\mathbf{r})f(\mathbf{r}) = k_0^2(1+v(\mathbf{r}))d(\mathbf{r}) \tag{A1}$$

with the boundary conditions

$$v^\delta(\mathbf{r}) = 0 \text{ on } L\cup L^-, \quad v^\delta(\mathbf{r}) + \frac{\partial v^\delta(\mathbf{r})}{\partial n} = 0 \text{ on } L^+. \tag{A2}$$

This equation is the Frechet derivative of the forward operator (3), which describes the forward propagation of light through the object. If $G^\delta(\mathbf{r},\mathbf{r}')$ is the Green's function associated with Eq. (A1), then the solution v^δ can be written as

$$v^\delta(\mathbf{r}) = \int_\Omega [G^v(\mathbf{r},\mathbf{r}')k_0^2(1+v(\mathbf{r}'))d(\mathbf{r}')]\mathrm{d}^n\mathbf{r}'. \tag{A3}$$

Multiplying Eq. (A1) by ψ belonging to the test function space and integrating over Ω, we have

$$\int_\Omega \bar{\psi}[\nabla\cdot\nabla v^\delta + 2ik_0\theta\cdot\nabla v^\delta - k_0^2 v^\delta f]\mathrm{d}^n\mathbf{r} = \int_\Omega \bar{\psi}[k_0^2(1+v)\mathrm{d}]\mathrm{d}^n\mathbf{r}. \tag{A4}$$

The first term on the left-hand side of Eq. (A4), on application of the divergence theorem, becomes

$$\int_\Omega \bar{\psi}[\nabla\cdot\nabla v^\delta]\mathrm{d}^n\mathbf{r} = \int_\Omega v^\delta[\nabla\cdot\nabla\bar{\psi}]\mathrm{d}^n\mathbf{r} - \int_{\partial\Omega} v^\delta\frac{\partial\bar{\psi}}{\partial n}\mathrm{d}^{n-1}\mathbf{r}. \tag{A5}$$

The second term can be written as

$$\int_\Omega (2ik_0\theta\cdot\nabla v^\delta)\bar{\psi}\mathrm{d}^n\mathbf{r} = -\int_\Omega (2ik_0\theta\cdot\nabla\bar{\psi})v^\delta\mathrm{d}^n\mathbf{r} + \int_{\partial\Omega} 2ik_0 v^\delta\bar{\psi}\theta\cdot n\mathrm{d}^{n-1}\mathbf{r}. \tag{A6}$$

Hence from Eq. (A4), we have

$$\int_\Omega \bar{\psi}[k_0^2(1+v)d]\mathrm{d}^n\mathbf{r} = \int_\Omega v^\delta[\nabla\cdot\nabla\bar{\psi} - 2ik_0\theta\cdot\nabla\bar{\psi} - k_0^2\bar{\psi}f]\mathrm{d}^n\mathbf{r}$$
$$- \int_{\partial\Omega} \frac{\partial\bar{\psi}}{\partial n} v^\delta \mathrm{d}^{n-1}\mathbf{r} + \int_{\partial\Omega} \frac{\partial v^\delta}{\partial n}\bar{\psi}\mathrm{d}^{n-1}\mathbf{r}$$
$$+ \int_{\partial\Omega} (2ik_0\theta\cdot n)v^\delta\bar{\psi}\mathrm{d}^{n-1}\mathbf{r}. \quad \text{(A7)}$$

Thus, if we choose ψ such that

$$\nabla\cdot\nabla\psi + 2ik_0\theta\cdot\nabla\psi - k_0^2\psi f = 0 \text{ on } \Omega \quad \text{(A8)}$$

with the boundary conditions

$$q^+ \equiv \frac{\partial\psi(\mathbf{r})}{\partial n} + \psi(\mathbf{r})(1+2ik_0\theta\cdot n) \text{ on } L^+,$$

$$\psi(\mathbf{r}) = 0 \text{ on } L\cup L^-, \quad \text{(A9)}$$

Eq. (A7) can be written as

$$\int_{L^+} \bar{q}^+ v^\delta \mathrm{d}r^{n-1} = -\int_\Omega \bar{\psi}[k_0^2(1+v)\mathrm{d}]\mathrm{d}^n\mathbf{r}. \quad \text{(A10)}$$

If q^+ is a delta function sitting on L^+, the boundary where the light is detected (and the light detector approximates the δ function), the left-hand side of Eq. (A10) picks out v^δ at the location $\mathbf{m}_0$ in L^+ of the δ function.

Therefore Eq. (A10) becomes

$$\int_\Omega \bar{\psi}[k_0^2(1+v)d]\mathrm{d}^n\mathbf{r} = -v^\delta(\mathbf{m}_0), \quad \mathbf{m}_0 \in L^+. \quad \text{(A11)}$$

Equation (A11) tells us that $v^\delta(\mathbf{r})$ is retrieved at the detector location $\mathbf{m}_0$, with the help of the integral on its left-hand side. This can be compared with Eq. (A3), which is the Green's function solution to the Frechet derivative equations (A1) and (A2). From this we see that ψ, which is the solution of Eqs. (A9) and (A10), acts like an adjoint Green's function of $G^v(\mathbf{r})$ in Eq. (A11) with the property that $\bar{G}^{(v)}_{adj}(\mathbf{r}',\mathbf{m}_0) = G^\phi(\mathbf{m}_0,\mathbf{r}')$. In this sense Eq. (A9) with the boundary condition in Eq. (A10) is the adjoint of the Frechet derivative given in Eqs. (A1) and (A2). The Jacobian elements are estimated from Eq. (A3) as

$$\frac{\partial v^\delta}{\partial d(\mathbf{r}')} = \bar{G}^{(v)}_{adj}k_0^2[1+v(\mathbf{r}')], \quad \forall\,\mathbf{r}'\in\Omega. \quad \text{(A12)}$$

To implement Eq. (A12) for all $\mathbf{r}'$, one needs to compute $v(\mathbf{r}')$ and $G^{(v)}_{adj}(\mathbf{r}',\mathbf{m}_0)$. First, $v(\mathbf{r}')$ is obtained by solving the equation for forward light propagation (3), and $G^{(v)}_{adj}(\mathbf{r}',\mathbf{m}_0)$ is obtained by solving the adjoint equation (A8), with the Robin source q^+ at $\mathbf{m}_0$. This helps one to compute the Jacobian for one view by solving two boundary value problems. In [6] the solution of the adjoint equation resulted in an update vector under the assumption that k_0 is large. This resulted in the propagation–backpropagation algorithm of [6]. But here the adjoint equation helps us compute the Jacobian matrix, with which a perturbation equation is set up, whose iterative solution results in the update vector.

REFERENCES

1. M. Soumekh and J. H. Choi, "Reconstruction in diffraction imaging," IEEE Trans. Ultrason. Ferroelectr. Freq. Control **36**, 93–100 (1989).
2. T. C. Wedberg and J. J. Stamnes, "Experimental examination of the quantitative imaging properties of optical diffraction tomography," J. Opt. Soc. Am. A **12**, 493–500 (1995).
3. S. Gutman and M. Klibanov, "Regularized quasi-Newton method for inverse scattering problems," Math. Comput. Modell. **18**, 5–31 (1993).
4. R. E. Kleinmann and P. M. Van den Berg, "Modified gradient method for 2-d problem in tomography," J. Comput. Appl. Math. **42**, 17–35 (1992).
5. A. C. Kak and M. Slaney, "Tomographic imaging with diffracting sources," in *Principles of Computerized Tomographic Imaging* (IEEE, 1988), pp. 211–217.
6. F. Natterer and F. Wübbeling, "A propagation-backpropagation method for ultrasound tomography," Inverse Probl. **11**, 1225–1232 (1995).
7. S. S. Cha and H. Sun, "Tomography for reconstructing continuous fields from ill-posed multidirectional interferometric data," Appl. Opt. **29**, 251–258 (1990).
8. T. E. Gureyev, A. Roberts, and K. A. Nugent, "Phase retrieval with the transport of intensity equation: matrix solution with use of zernite polynomial," J. Opt. Soc. Am. A **12**, 1932–1941 (1995).
9. K. Ichikawa, A. W. Lohmann, and M. Takeda, "Phase retrieval based on the irradiance transport equation and the Fourier transform method: experiments," Appl. Opt. **27**, 3433–3436 (1988).
10. T. C. Wedberg and J. J. Stamnes, "Comparison of phase retrieval methods in optical diffraction tomography," Pure Appl. Opt. **4**, 39–54 (1995).
11. A. Barty, K. A. Nugent, D. Paganin, and A. Roberts, "Quantitative optical phase microscopy," Opt. Lett. **23**, 817–819 (1998).
12. G. Gbur and E. Wolf, "Hybrid diffraction tomography without phase information," J. Opt. Soc. Am. A **19**, 2194–2202 (2002).
13. M. H. Maleki and A. J. Devaney, "Phase retrieval and intensity-only reconstruction algorithms for optical diffraction tomography," J. Opt. Soc. Am. A **10**, 1086–1092 (1993).
14. J. Cheng and S. Han, "Diffraction tomography reconstruction algorithms for quantitative imaging of phase objects," J. Opt. Soc. Am. A **18**, 1460–1464 (2001).
15. M. H. Maleki, A. J. Devaney, and A. Schatzberg, "Tomographic reconstruction from optical scattered intensities," J. Opt. Soc. Am. A **9**, 1356–1363 (1992).
16. M. R. Teague, "Deterministic phase retrieval: a Green's function solution," J. Opt. Soc. Am. **73**, 1434–1441 (1983).
17. G. Vdovin, "Reconstrution of an object shape from the near-field intensity of a reflected paraxial beam," Appl. Opt. **36**, 5508–5513 (1997).
18. N. Jayashree, G. Keshava Datta, and R. M. Vasu, "Optical tomographic microscope for quantitaive imaging of phase objects," Appl. Opt. **39**, 277–283 (2000).
19. K. A. Nugent, T. E. Gureyev, D. F. Cookson, D. Paganin, and Z. Barnea, "Quantitative phase imaging using hard x-rays," Phys. Rev. Lett. **77**, 2961–2964 (1996).
20. A. Semichaevsky and M. Testorf, "Phase-space interpretation of deterministic phase retrieval," J. Opt. Soc. Am. A **21**, 2173–2179 (2004).
21. A. H. Hielscher, A. D. Klose, and K. M. Hansen, "Gradient-based iterative image reconstruction scheme for time-resolved optical tomography," IEEE Trans. Med. Imaging **18**, 262–271 (1999).
22. S. R. Arridge and M. Schweiger, "A gradient based optimization scheme for optical tomography," Opt. Express **6**, 213–226 (1998).
23. S. R. Arridge, "Topical review: optical tomography in medical imaging," Inverse Probl. **15**, R41–R93 (1999).
24. S. R. Arridge, "Photon-measurement density functions. Part 1: analytical forms," Appl. Opt. **34**, 7395–7409 (1995).

25. S. R. Arridge, "Photon-measurement density functions. Part 2: finite-element-method calculations," Appl. Opt. **34**, 8026–8037 (1995).
26. B. Kanmani and R. M. Vasu, "Diffuse optical tomography through solving a system of quadratic equation: theory and simulation," Phys. Med. Biol. **51**, 981–998 (2006).
27. J. Shen and L. L. Wang, "Spectral approximation of the Helmholtz equation with high wave numbers," SIAM (Soc. Ind. Appl. Math.) J. Numer. Anal. **43**, 623–644 (2005).
28. S. Chandler-Wilde and S. Langdon, "A wave number independent boundary element method for an acoustic scattering problem," SIAM (Soc. Ind. Appl. Math.) J. Numer. Anal. **43**, 2450–2477 (2006).
29. S. Kim, C. S. Shin, and J. B. Keller, "High-frequency asymptotics for the numerical solution of Helmholtz equation," Appl. Math. Lett. **18**, 797–804 (2005).
30. F. Natterer, "Marching schemes for inverse Helmholtz and Maxwell problems," http://arachne.uni-muenster.de:8000/num/Preprints.
31. W. Dahmen, "Wavelet and multiscale methods for operator equations," Acta Numerica **6**, 55–228 (1997).